AIAA JOURNAL
Vol. 37, No. 6, June 1999

Technical Notes

TECHNICAL NOTES are short manuscripts describing new developments or important results of a preliminary nature. These Notes cannot exceed 6 manuscript pages and 3 figures; a page of text may be substituted for a figure and vice versa. After informal review by the editors, they may be published within a few months of the date of receipt. Style requirements are the same as for regular contributions (see inside back cover).

Robust Implicit Multigrid Method for the Simulation of Turbulent Supersonic Mixing

P. Gerlinger,* P. Stoll,† and D. Brüggemann‡
University of Stuttgart, 70550 Stuttgart, Germany

Introduction

DURING the past few years, considerable progress has been achieved in employing multigrid methods for turbulent supersonic and hypersonic flows.[1–7] In this context, the most serious problems arise from strongly nonlinear turbulent source terms of low-Reynolds-number turbulence models and from the hyperbolic character of the governing equations in high-speed flows. Because of the relatively weak coupling between fluid and turbulence variables, a simple coarse-grid freezing of nonlinear contributions to the turbulent source vector enables convergence even in complicated cases.[6,7] In addition, supersonic flows require modifications of standard restriction and prolongation operators to avoid upwind influences at shock waves. Koren and Hemker[8] proposed a local defect damping and a direction-dependent prolongation. Without defect damping but using characteristic restriction and prolongation operators, good convergence rates could be achieved for the Euler equations at hypersonic flight conditions by Leclercq and Stoufflet.[9] Both methods are computationally expensive. In this Note, we present a modified simple defect damping and prolongation procedure that is easy to implement and that works stably even for high-aspect-ratio grids. A novel blending between first-order upwind prolongation and second-order central prolongation improves robustness, as well as the convergence rate of the algorithm. With this technique, the reduction to first-order accuracy is limited to the vicinity of shock waves. A general drawback of these restriction and prolongation operators is the dependence on free parameters. However, it is shown that the influence of the choice of these parameters is quite weak and that the presented method may also be used for complicated engineering problems. A reduction in CPU time by a factor of four is achieved simulating a turbulent supersonic mixing experiment.

Received May 14, 1997; revision received Nov. 30, 1998; accepted for publication Feb. 6, 1999.

*Research Scientist, Institut für Thermodynamik der Luft- und Raumfahrt, Pfaffenwaldring 31. E-mail: peter.gerlinger@itlr.uni-stuttgart.de. Member AIAA.

†Research Scientist, Institut für Thermodynamik der Luft- und Raumfahrt, Pfaffenwaldring 31. E-mail: peter.stoll@itlr.uni-stuttgart.de. Member AIAA.

‡Professor, Institut für Thermodynamik der Luft- und Raumfahrt, Pfaffenwaldring 31. E-mail: dieter.brueggemann@itlr.uni-stuttgart.de.

Multigrid Method

A nested full approximation storage (FAS), V-cycle multigrid method[10] for nonlinear problems is used as convergence acceleration for solving the full Navier–Stokes, species and turbulence transport equations. Full coarsening is performed on four grid levels. Details concerning the implicit numerical scheme and the treatment of turbulent source terms of the employed low-Reynolds-number q–ω turbulence closure may be found in Refs. 6 and 7.

Restriction

If strong shock waves occur in the flowfield, central restriction operators lead to unphysical upwind influences, which usually destroy convergence of multigrid methods. Koren and Hemker[8] have shown that one possibility to overcome stability problems is a local damping of the transferred residual error at shock waves. However, the proposed local damping factor requires calculation of different matrix norms and is, consequently, computationally expensive, especially for multicomponent flows. On the other hand, a simple global damping, also used by some authors, destroys much of the information restricted to coarser grids, thus retarding convergence. Therefore, it is advantageous to damp the transferred residual error at shock waves only. It will be shown that the extent of damping is actually rather small and insensitive to the choice of damping parameters. In the present Note, a shock sensor similar to that used in Ref. 3 is used to reduce the transferred residual error. In contrast to Ref. 3, the present sensor[11] is a blend $0 \le \chi \le 1$ between a standard non-total variational diminishing (TVD) sensor ($\chi = 1$) and a sensor with TVD properties ($\chi = 0$), which offers better convergence rates at high Mach numbers. For the ξ direction, this sensor is given by

$$\nu^{\xi}_{i,j} = \frac{|p_{i+1,j} - 2p_{i,j} + p_{i-1,j}|}{(1-\chi)(|p_{i+1,j} - p_{i,j}| + |p_{i,j} - p_{i-1,j}|) + \chi(p_{i+1,j} + 2p_{i,j} + p_{i-1,j})} \tag{1}$$

where a value of $\chi = 0.8$ resulted in good shock resolution and convergence histories. On the basis of this shock sensor, the coarse-grid damping factor is calculated by

$$\kappa^{k}_{i,j} = \max\Big[0, 1 - C^{k}\max\Big(\nu^{\xi}_{i,j}, \nu^{\xi}_{i-1,j}, \nu^{\xi}_{i+1,j}, \nu^{\eta}_{i,j}, \nu^{\eta}_{i,j-1}, \nu^{\eta}_{i,j+1}\Big)\Big] \tag{2}$$

where k indicates the grid level. Instead of adding up four fine-grid residuals $\boldsymbol{R}$ to form one coarse-grid residual, the following transfer operator is used:

$$r^{k+1}_{k}\boldsymbol{R}^{k} = \sum_{l=1}^{4} \boldsymbol{R}^{k}_{l}\max\Big(0, 1 - \kappa^{k}_{l}\Big) \tag{3}$$

In smooth regions of the flowfield, $\kappa^{k}_{i,j}$ is close to zero and the total residual error is restricted to the next coarser grid. Near shock waves, $\kappa^{k}_{i,j}$ increases and the transferred residual error is consequently reduced. The coefficients C^{k} should be chosen in dependence of parameter χ. Although for the more dissipative pure TVD sensor ($\chi = 0$) ν is close to 1 in the vicinity of shock waves, its value strongly decreases with blending to the non-TVD sensor. Therefore, higher values of C^{k} are necessary for the non-TVD sensor.

An intermediate sensor ($\chi = 0.8$) is used in the present Note. For a great variety of different test cases, good results are obtained with $0.5 \leq C^k \leq 2$, where high values are necessary to simulate strong shock waves. Fortunately, the influence of C^k on convergence history is only moderate if it does not fall below a lower limit. In practice it was possible to simulate a wide range of flow problems with the same set of coefficients. Also note that often small reductions in the transferred residual errors at shock waves (approximately 10% for transfer from first to second grid) are sufficient to allow the multigrid method to converge.

Prolongation

Prolongation of coarse-grid corrections to finer grids is usually performed by a spatially second-order bilinear interpolation. Figure 1 shows four coarse-grid cell centers (1–4) that are used to determine fine-grid values A–D. Before starting the iteration process, four prolongation factors P_i

$$\sum_{i=1}^{4} P_i = 1$$

are calculated for every fine-grid cell center. Using these prolongation factors, the coarse-grid correction for cell center A is

$$\Delta \boldsymbol{Q}_A^k = \sum_{i=1}^{4} P_i \Delta \boldsymbol{Q}_i^{k+1} \tag{4}$$

In the case of highly stretched curvilinear grids, problems may arise (Fig. 2) if fine-grid cell centers (A–D) are located outside of corresponding coarse-grid cell centers. In this case large errors result from extrapolation. To avoid such problems, the four fine-grid cell centers are first transformed to the coarse grid. The fine-grid corrections are then determined for the fictious cell centers A^*–D^*, thus eluding problems from extrapolation.

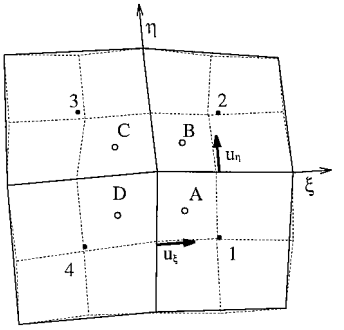

Fig. 1 Geometry with coarse- (●) and fine- (○) grid cell centers.

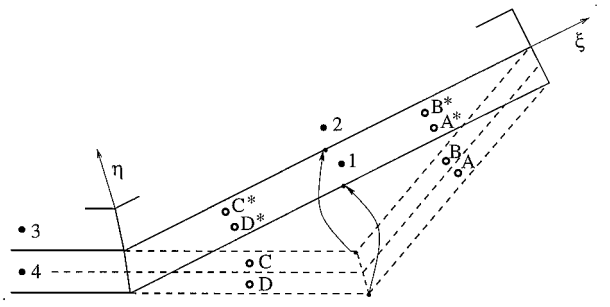

Fig. 2 Schematic of prolongation on highly stretched grids.

Such a bilinear prolongation operator leads to upwind influences at shock waves, too. In Ref. 7 a simple form of a pure upwind prolongation is used in supersonic regions of the flowfield. If, for example, the contravariant velocity $|u_\xi|$ (Fig. 1) between the coarse-grid cell centers 4 and 1 is smaller than 1, central prolongation is used. If $|u_\xi|$ is larger than 1, only the coarse-grid value located upstream is considered. The disadvantage of this method is the reduction from second- to first-order accuracy in supersonic parts of the flowfield. In some investigated cases, this kind of prolongation failed to achieve convergence. This problem is alleviated by the following modification: The corrections $\Delta \boldsymbol{Q}^{k+1}$ in Eq. (4) are replaced by new values, which account for upwind influences. For example, for the coarse-grid cell center 1, the new correction is calculated by

$$\Delta \boldsymbol{Q}_{1,\text{new}}^{k+1} = \Delta \boldsymbol{Q}_1^{k+1} + a\left[\kappa_\xi\left(\Delta \boldsymbol{Q}_4^{k+1} - \Delta \boldsymbol{Q}_1^{k+1}\right) + \kappa_\eta\left(\Delta \boldsymbol{Q}_2^{k+1} - \Delta \boldsymbol{Q}_1^{k+1}\right)\right] \tag{5}$$

with

$$\kappa_\xi = \begin{cases} \nu^\xi : u_\xi > 1 \\ 0 : u_\xi \leq 1 \end{cases}, \qquad \kappa_\eta = \begin{cases} \nu^\eta : u_\eta < -1 \\ 0 : u_\eta \geq -1 \end{cases} \tag{6}$$

and $a = 0.5$ if both κ_ξ and $\kappa_\eta \neq 0$, whereas $a = 1$ in all other cases. The pressure sensors ν in the ξ and η directions [see Eq. (1)] are used to blend between central and upwind prolongation. Thus, first-order upwind prolongation is performed near shock waves only, where ν is larger than 0 and may approach 1. In subsonic or smooth supersonic flow regions, $\nu \approx 0$ and the second-order central prolongation is retained.

Results and Discussion

Several supersonic mixing test cases[12] are simulated to investigate the efficiency of the described restriction and prolongation operators. Cold hydrogen is injected through the blunt end of a strut into a Mach 2 supersonic airflow. A three-block grid with 328×32, 288×56, and 480×96 volumes is used to discretize the upper part of the symmetric channel. A second nozzle for hydrogen injection inside the strut is simulated with 40 volumes in the streamwise direction. Figure 3 shows calculated pressure contours for the upstream located channel part. A detailed description, as well as a comparison with experimental data, is given in Ref. 12. This test case offers several challenges to multigrid methods, such as shock waves, a recirculation zone at the blunt end of the strut, strong density gradients within the hydrogen/air shear layer, large turbulent production, and high cell aspect ratios of up to 7100. Pure upwind prolongation failed for this test case. The results shown in Fig. 4 were obtained using the alternative prolongation operator of Eq. (5). Plotted are convergence histories of the density and turbulence ($q = \sqrt{k}$, where k = turbulent kinetic energy) residuals vs the number of work units. One work unit is defined as the computational time needed for one fine-grid iteration. Additionally, the influence of a variation of restriction damping parameter C^k [see Eq. (2)] is included. For simplicity this investigation was performed with the same value of $C^k = C$ at all grid levels. Without damping of the restricted residual error, the calculation already failed during the nested iteration process. The best convergence rate is obtained for $C = 2$. Whereas a higher value ($C = 3$) has only slight influence on the convergence behavior, smaller values ($C = 1$) considerably degrade the rate of convergence. For the calculation with $C = 2$, the maximum value of κ out of all grid volumes is 0.114, 0.184, and 0.318 for the transfer from first to second, second to third, and third to fourth level, respectively.

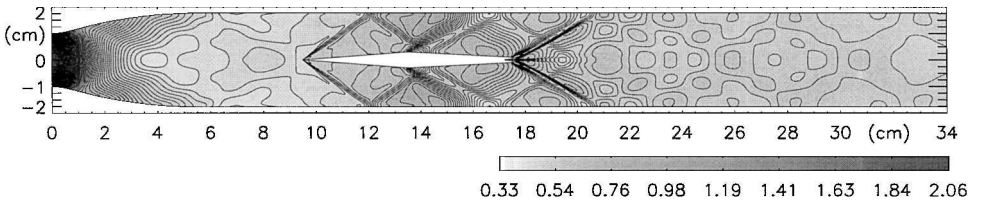

Fig. 3 Pressure contours (bar).

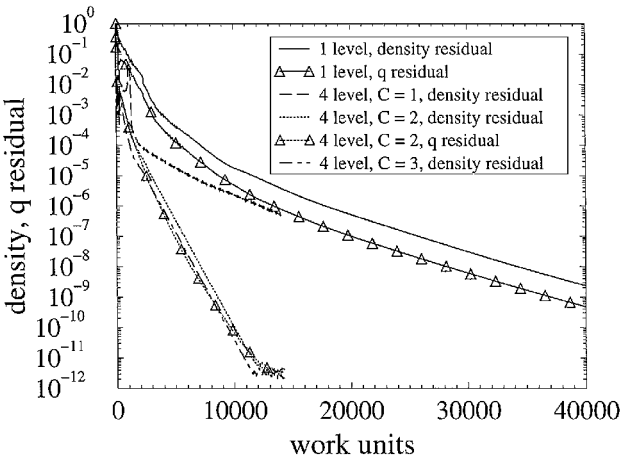

Fig. 4 Convergence history for density and turbulence residuals.

Conclusions

Some modifications for the restriction and prolongation process of multigrid methods have been presented that are necessary for the simulation of complex supersonic flowfields. Damping of the restricted residual error and blending between a second-order central and a first-order upwind prolongation enable convergence in supersonic flows and resulted in strong reductions in CPU time. The advantage of this kind of blending is the reduction to first-order prolongation at shock waves only.

Acknowledgments

We wish to thank the Deutsche Forschungsgemeinschaft for financial support of this work within the Collaborative Research Center SFB 259 at the University of Stuttgart.

References

[1]Turkel, E., Swanson, R. C., Vatsa, V. N., and White, V. N., "Multigrid for Hypersonic Viscous Two- and Three-Dimensional Flow," Inst. for Computer Applications in Science and Engineering, ICASE Rept. 91-57, Contract NAS1-18605, Hampton, VA, July 1991.

[2]Vatsa, V. N., Turkel, E., and Abolhassani, J. S., "Extension of Multigrid Methodology to Supersonic/Hypersonic 3-D Viscous Flows," *International Journal for Numerical Methods in Fluids*, Vol. 17, No. 10, 1993, pp. 825–837.

[3]Radespiel, R., and Swanson, R. C., "Progress with Multigrid Schemes for Hypersonic Flow Problems," *Journal of Computational Physics*, Vol. 116, Jan. 1995, pp. 103–122.

[4]Edwards, J. R., "Development of an Upwind Relaxation Multigrid Method for Computing Three-Dimensional Viscous Internal Flows," AIAA Paper 95-0208, Jan. 1995.

[5]Liu, F., and Shanhong, J., "Unsteady Flow Calculations with a Multigrid Navier–Stokes Method," *AIAA Journal*, Vol. 34, No. 10, 1996, pp. 2047–2053.

[6]Gerlinger, P., and Brüggemann, D., "Multigrid Convergence Acceleration for Turbulent Supersonic Flows," *International Journal for Numerical Methods in Fluids*, Vol. 24, No. 10, 1997, pp. 1019–1035.

[7]Gerlinger, P., and Brüggemann, D., "An Implicit Multigrid Scheme for the Compressible Navier–Stokes Equations with Low-Reynolds-Number Turbulence Closure," *Journal of Fluids Engineering*, Vol. 120, June 1998, pp. 257–262.

[8]Koren, B., and Hemker, P. W., "Damped, Direction-Dependent Multigrid for Hypersonic Flow Computations," *Applied Numerical Mathematics*, Vol. 7, April 1991, pp. 309–328.

[9]Leclercq, M. P., and Stoufflet, B., "Characteristic Multigrid Method to Solve the Euler Equations with Unstructured and Nested Grids," *Journal of Computational Physics*, Vol. 104, Feb. 1993, pp. 329–346.

[10]Jameson, A., and Yoon, S., "Lower–Upper Implicit Schemes with Multiple Grids for the Euler Equations," *AIAA Journal*, Vol. 25, No. 7, 1987, pp. 929–935.

[11]Swanson, R. C., and Turkel, E., "On Central Difference and Upwind Schemes," *Journal of Computational Physics*, Vol. 101, Aug. 1992, pp. 292–306.

[12]Gerlinger, P., Kasal, P., Boltz, J., and Brüggemann, D., "Numerical Investigation of Hydrogen Strut Injections into Supersonic Air Flows," AIAA Paper 98-3424, July 1998.

D. S. McRae
Associate Editor

Elliptic Grid Generation

Reijo Lehtimäki*
Helsinki University of Technology,
FIN-02015 HUT, Espoo, Finland

Introduction

GRID generation is an essential part of computational fluid dynamics. Structured multiblock grids can already in practice be generated into remarkably complex geometries. Grid generation is, however, a task that demands a major share of the man hours spent on the flow solution and that remains a research subject of practical interest.

In the two-dimensional case, the harmonic map is a diffeomorphism. Unfortunately, it seems this result cannot be generalized to three space dimensions.[1] Furthermore, the theorems are for the continuous map, and it is the discrete approximation that forms the grid. Yet the harmonic method is in practice very robust. Unfortunately, a straightforward application of the Laplace–Beltrami equation does not allow any control of the grid, but the grid always becomes evenly spaced in the interior. A common approach is to add an inhomogeneous term to the equation and to use this inhomogeneous equation, the Poisson equation, for grid generation.[2] One technique for calculating the control terms is to apply an intermediate parameter domain.[3] There are a number of other techniques as well, in which the Poisson system is applied without any concern about the regularity of the parameter domain to which the control terms possibly correspond. Methods based on the Beltrami equation directly, without any control terms, have also been developed. For example, Dvinsky applies predefined metrics in the physical domain to achieve grid control.[4]

In the present method, grid clustering is achieved via a clustered computational domain from which nonuniform difference increments are calculated in the discretization of the Laplace equation. The method does not include grid orthogonalization. The generated grid can be orthogonalized to the boundary afterward.[5] In fact, any orthogonalization requirements would make the grid-generation problem overdetermined.[5] Thus, adding an orthogonalization feature to the method, e.g., by adjusting the computational domain further, would probably lessen the robustness of the method.

Grid-Generation Equations

Harmonic maps are extremals of the energy functional. Consider a harmonic map from the physical to the computational domain. Suppose the computational space is a Euclidean space equipped with a Cartesian coordinate system ξ^n. If the physical space is also a Euclidean space and the coordinate system x^n Cartesian, then the Euler equation for the energy functional reduces to the Laplace equation. In the case of a nonvanishing Jacobian, the Laplace equation can be transformed so that the curvilinear coordinates appear as independent variables and the Cartesian coordinates as dependent[2]:

$$g^{kj}\frac{\partial^2 x^\lambda}{\partial\xi^k\partial\xi^j} = 0 \tag{1}$$

Here the g^{kj} are the contravariant components of the metric tensor of the coordinate system on the physical space induced by the harmonic map. Equation (1) is the grid-generation equation for two- and three-dimensional flat domains.

If the physical space is a curved surface in a three-dimensional Euclidean space, the application of the formulas of Gauss yields the harmonic grid-generation equation on a surface[2,6]:

$$g^{kj}\frac{\partial^2 x^\lambda}{\partial\xi^k\partial\xi^j} = G(K_1 + K_2)n^\lambda \tag{2}$$

Received Nov. 26, 1997; revision received Jan. 25, 1999; accepted for publication Jan. 29, 1999.

*Research Scientist, Laboratory of Aerodynamics, P.O. Box 4400.